Semiconductor Physics, Quantum Electronics & Optoelectronics, 2021. V. 24, No 4. P. 378-389.

Thermal annealing ambiance effect on phosphorus passivation and reactivation mechanisms in silicon-based Schottky diodes hydrogenated by MW-ECR plasma

D. Belfennache[1,*], D. Madi[2], R. Yekhlef[1], L. Toukal[3], N. Maouche[3], M.S. Akhtar[4], S. Zahra[4]

[1]*Research Center in Industrial Technologies CRTI, P.O. Box 64, Cheraga, 16014 Algiers, Algeria*
[2]*Physics Department, Bouira University, P.O. Box 1000, Street of Independence, Bouira, Algeria*
[3]*Laboratory of Electrochemistry and Materials University of Sétif, 1900, Algeria*
[4]*Department of Physics, Division of Science and Technology, University of Education, Lahore, Pakistan*
[*]*Corresponding author email: belfennachedjamel@gmail.com*

Abstract. The main objective of this work is to investigate the effect of thermal annealing in forming gas atmosphere on the mechanism of deactivation and reactivation of phosphorus in silicon-based Schottky diodes. Firstly, the microwave plasma power, initial phosphorus concentration in the samples and hydrogen flux were fixed as 650 W, 10^{15} cm^{-3}, and 30 sccm, respectively, to investigate the behavior of different working parameters of diodes, specifically the duration and temperature of hydrogenation. Secondly, few samples hydrogenated at 400 °C for 1 h were annealed under the forming gas (10% H_2 + 90% N_2) within the temperature range from 100 to 700 °C for 1 h. The profiles of active phosphorus concentration were monitored by evaluating the change in concentration of phosphorus after hydrogenation or thermal annealing in a forming gas environment through capacitance-voltage measurements. The obtained results depict the temperature and duration of hydrogenation, which ultimately reveals the complex behavior of phosphorous and hydrogen in silicon. However, the phosphorus passivation rate is homogeneous over all the depths measured at 400 °C. The thermal annealing in a forming gas indicates the increase in passivation rate of phosphorus as a function of annealing temperature, till the passivation rate attains saturation in the sample annealed at 400 °C. At higher temperatures, a decrease in the concentration of phosphorous-hydrogen complexes is observed due to the dissociation of these complexes and reactivation of phosphorus under thermal effect.

Keywords: phosphorus passivation, plasma hydrogenation, thermal annealing, forming gas.

https://doi.org/10.15407/spqeo24.04.378
PACS 81.65.Rv, 85.30.Kk

Manuscript received 14.07.21; revised version received 10.08.21; accepted for publication 10.11.21;

1. Introduction

In the recent century, hydrogen has caused great interest in semiconductors, especially silicon, with the discovery that the incorporation of H has dramatically improved the properties of Si [1, 2]. However, the properties of hydrogen in silicon are still not well understood [3–5]. This is mainly due to the complex behavior of hydrogen in silicon and its ability to passivate crystalline defects in it and react with dopant to form inactive complexes [6]. A simple example that remains under attention of researchers is the hydrogen passivation of doping atoms in silicon, leading to an increase in the resistivity of the material [7, 8]. The discovery of these phenomena causes a veritable explosion of research activity to study their impacts in the technological environment, in particular, in the photovoltaic field [9, 10]. Also, the process of annealing in forming gas (FG) is a widely established and industrially well-applied mechanism for passivating crystalline silicon films [11]. Capacitance-voltage (*C–V*) measurement is an approved methodology to investigate the variation in dopants concentration in silicon-based Schottky diodes [12, 13]. In the standard manufacturing process for photovoltaic cells, hydrogen comes mainly from the anti-reflective and passivating layer on the surface of solar cell emitters [13, 14]. The realization of a high-efficiency photovoltaic cell is one of the major problems that technologists are faced [15–18].

Some researchers [19, 20] have reported that the performance of many in expensive silicon solar cells improves upon annealing in forming gas atmosphere and that hydrogen is responsible for the improvement. Consequently, it is essential to carry out researches in terms of H diffusion and defect passivation in Si to produce photovoltaic converters with better yields.

For polycrystalline material, a higher concentration of defects at the grain boundaries would lead to lower photovoltaic efficiency of a cell with an n^+-p-p^+ structure, as compared to that of monocrystalline silicon. Therefore, several procedures were performed to deactivate these defects by introducing hydrogen into the n^+-p-p^+ cell. However, passivation of defects in polysilicon belongs to the n^+-emitter region doped with phosphorus [21]. To study the effect of the ambiance under thermal annealing on phosphorus in hydrogenated monosilicon is the main focus of this research, since it is free from defects and can be used as a base material for the Schottky diode. Using capacitance and voltage measurements, phosphorus doping profiles are extracted during the annealing process. Heat treatment at these temperatures also leads to dissociation of hydrogen-defect complexes and reactivation of defects. Moreover, the effect of hydrogen on phosphorus deactivation of various initial phosphorus concentrations was studied and mentioned in our previous publication [22]. It has been observed that the doping profile is never uniform in silicon and especially at surfaces and interfaces due to the introduction of hydrogen during hydrogenation processes. Since the electrical properties of silicon can be controlled by the type of dopant and doping profile. However, the mechanism for neutralizing phosphorus in silicon is still not clearly defined. Therefore, it is interesting to see the effects of the environment of thermal annealing on the mechanisms of passivation and reactivation of phosphorus in monosilicon. The purpose of this work is to investigate the thermal annealing ambiance effect of phosphorus passivation and reactivation in silicon-based Schottky diodes. The microwave cyclotron electron resonance (MW-ECR) system was employed to investigate the variability of numerous diode operating parameters before and after hydrogenation *via* *C–V* values.

2. Phosphorus deactivation and reactivation mechanisms

Passivation and reactivation of phosphorus in silicon by hydrogen is well ascertained, the mechanism by which it occurs remains a more common focus of attention [23]. In the case of treatment in hydrogen plasma, the mechanism of passivation of the phosphorus atoms involves the change in charge from positive to negative for hydrogen occurred at ambient temperature as it follows.

H^+ captures an electron to form H^0, then H^0 captures second electron to produce hydrogen H^- or capture another H^0 to form its molecule H_2:

$$\mathrm{H}^+ + \mathrm{e}^- \to \mathrm{H}^0, \tag{1}$$

$$\mathrm{H}^0 + \mathrm{e}^- \to \mathrm{H}^-, \tag{2}$$

$$\mathrm{H}^0 + \mathrm{H}^0 \to \mathrm{H}_2. \tag{3}$$

Migration of H^0 species cannot contribute to the neutralization of phosphorus atoms while the migration of dissociated hydrogen as H^-, followed by an interaction of electrostatic origin between H^- and P^+ ions to form a neutral complex of the hydrogen–phosphor (PH) type:

$$\mathrm{H}^0 + \mathrm{P}^+ \xrightarrow{K_{\mathrm{PH}}} \mathrm{PH}. \tag{4}$$

The thermal dissociation of the PH complexes is expressed by the following initial reaction:

$$\mathrm{PH} \xrightarrow{K'_{\mathrm{PH}}} \mathrm{P}^+ + \mathrm{H}^-. \tag{5}$$

Here, K_{PH} (K'_{PH}) represents the coefficient of mobile hydrogen combination (dissociation) with phosphorus atoms.

After this partial dissociation, H^- absorbs a hole to become H^0, as follows:

$$\mathrm{H}^- + h^+ \to \mathrm{H}^0. \tag{6}$$

Therefore, for *n*-type silicon, hydrogen exists in two associated states of charge, H^- and H^0. K'_{PH} represents the coefficient of mobile hydrogen dissociation with phosphorus atoms. These reversible reactions are characterized by the diffusion coefficients D_{H^-} defined by the following relation:

$$x_{\mathrm{H}^-} = \sqrt{D_{\mathrm{H}^-} \cdot t_{\mathrm{H}}}, \tag{7}$$

where D_{H^-} is the diffusion coefficient of H^-, x_{H^-} is its diffusion depth, and t_{H} – hydrogenation time.

The relative concentration of two associated states of charge at the Fermi level can be determined by the following relation:

$$\frac{\left[\mathrm{H}^-\right]}{\left[\mathrm{H}^0\right]} = \exp\left[\frac{E_{\mathrm{F}} - E_a}{k_{\mathrm{B}}T}\right]. \tag{8}$$

Here, E_a, E_{F}, T, and K_{B} represent the acceptor energy level, Fermi level, temperature and the Boltzmann constant, respectively.

At room temperature, if all the phosphorus atoms are ionized, the concentration of active phosphorus is the same as the total concentration of phosphorus. However, after the hydrogenation process, the total concentration of phosphorus is expressed as follows:

$$\left[\mathrm{P}_{\mathrm{total}}\right] = \left[\mathrm{P}^+\right] + \left[\mathrm{PH}\right]. \tag{9}$$

Using the relation (9), evolution of the inactive concentration of phosphorus can be expressed like that:

$$\left[\mathrm{PH}\right] = \left[\mathrm{P}_{\mathrm{total}}\right] - \left[\mathrm{P}^+\right]. \tag{10}$$

Given that H^0 and H^- are mobile, the total flow of H is caused by the individual contribution of H^0 and H^- expressed according to Fick's first law:

$$J_{\mathrm{H}^0} = -D_{\mathrm{H}^-}\frac{\partial \mathrm{H}^0}{\partial x}, \qquad (11)$$

$$J_{\mathrm{H}^-} = -D_{\mathrm{H}^-}\frac{\partial\left[\mathrm{H}^-\right]}{\partial x} + D_{\mathrm{H}^-}\left[\mathrm{H}^-\right]\frac{1}{n}\cdot\frac{\partial n}{\partial x}. \qquad (12)$$

The last term in the equation (11) returns to the local density of free carriers and the combined electric field. By solving the Poisson equation, n can be determined.

Evolution of a diverse concentration can be calculated through the following equation system:

$$\frac{\partial[\mathrm{H}]^{tot}}{\partial t} = -\frac{\partial\left[J_{\mathrm{H}^0} + J_{\mathrm{H}^-}\right]}{\partial x}, \qquad (13)$$

$$\frac{\partial[\mathrm{PH}]}{\partial t} = K_{\mathrm{PH}}\left[\mathrm{P}^+\right]\left[\mathrm{H}^-\right] - K'_{\mathrm{PH}}[\mathrm{PH}]. \qquad (14)$$

Here, $[\mathrm{H}]^{tot}$ is the total concentration of hydrogen including $[\mathrm{H}^0]$, $[\mathrm{H}^-]$, [PH] and other trapped hydrogen [T, H] available on surface defects in the form of platelets due to damage caused by plasma [20].

3. *C–V* profiling of phosphorus *n*-type silicon

The *C–V* method describes the dependence of arial space width on the applied reverse bias voltages that ultimately decide the viability of metal/semiconductor structure (Schottky diodes) or n^+-p (*p-n* junctions) and metal-oxide-semiconductor (MOS) [24]. In this section, the derivations and equations required to extract doping profile by the *C–V* method will be discussed briefly.

$$C = \frac{dQ_s}{dV}, \qquad (15)$$

where dQ_s is the change in charge in the depletion space-charge region, per unit area caused by a change dV in the applied voltage.

Based on the semiconductor neutrality, the equation can be approximated by:

$$dQ_s = qAN_A(w)dw. \qquad (16)$$

The combination of the equations (15) and (16) gives rise to dN_A/dV:

$$C = \frac{dQ_s}{dV} = qAN_A(w)dw. \qquad (17)$$

The equation (17) is obtained by neglecting the term dN_A/dV or by assuming it to be zero. This assumption means that N_A does not vary beyond the distance w.

The cause for dQ_s is primarily alterations in charges associated with shallow donors near the depletion region edge so that, under the depletion approximation and by neglecting the contribution from deep states, the depletion region capacitance can be expressed as [25]

$$C = -\frac{K_S\varepsilon_0 A}{w}, \qquad (18)$$

where $K_S\varepsilon_0 = 11.7\cdot 8.85\cdot 10^{-1}$ F/m, A is the junction area and w is the width of space load zone. K_S and ε_0 are the dielectric constant of silicon and the permittivity of vacuum, respectively.

The differentiation of the equation (18) with respect to the voltage and the substitution of the term (dw/dV) in the equation (17) give rise to the following equation:

$$N_A(w) = -\frac{C^2}{qK_S\varepsilon_0 A^2[dC/dV]}. \qquad (19)$$

The equation (19) can be also rewritten as

$$N_A(w) = -\frac{2}{qK_S\varepsilon_0 A^2\left[\frac{d\left(1/C^2\right)}{dV}\right]}. \qquad (20)$$

Finally, the processing of the experimental data related to the capacitance-voltage characteristic curve with the equations (18), (19) or (20) is sufficient to extract the doping profile.

4. Experimental procedure

The samples were monocrystalline silicon films obtained using the zone melting method (FZ) with the crystallographic direction ⟨100⟩ and 300 µm in thickness. They were in the form of square plates 15×15 mm^2, having received during their production 10^{15} cm^{-3} doping in phosphorus of *n*-type (P-Si). On P-Si films, diodes of Schottky structures have been developed. The silicon films were first hydrogenated in the microwave discharge reactor assisted by electron cyclotron resonance. Discharged from the "Microsys 400 PECVD" reactor. MW-ECR a schematic diagram of the experimental apparatus is shown in Fig. 1.

The hydrogen gas was excited by 2.45-GHz microwaves in the resonant chamber, to maintain the ECR state the magnetic field was applied. The gas pressure in the plasma was 0.6 Pa at a hydrogen (H_2) flow rate of 30 sccm^2 and hydrogenation energy of 650 W. The duration and temperature of hydrogenation varied from one to two hours and from 50 to 500 °C, respectively. Thermal annealing of some samples was performed in a (10% H_2 + 90% N_2) FG atmosphere for the temperature range of 100 to 700 °C for 1 h. The input MW power and reflection (<5%) were analyzed for all cases. In the cooling phase, to avoid hydrogen diffusion, the plasma was kept for 10…20 min until the substrate temperature approaches 280 °C. They are cleaned in a bath of hydrofluoric acid HF (2%) for 2 min followed by rinsing with deionized water and finally dried under a stream of nitrogen. On the hydrogenated faces, we have applied a mask with square openings of 1×1 mm^2 and separated them from each other by a distance of 1 mm.

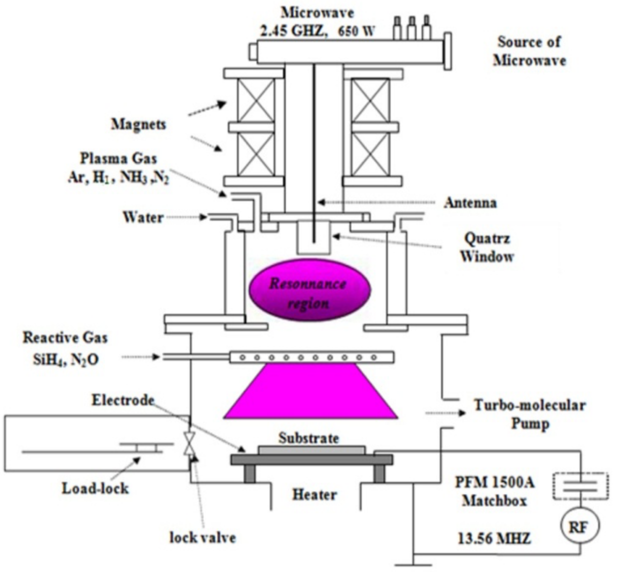

Fig. 1. Schematic of the ECR-PECVD reactor used in this study.

This step was followed by the introduction of the samples into a Joule effect thermal evaporator to deposit a layer of gold (Au), with a cross-section of 1×1 mm^2 and 0.1-µm thick, on the one hand, through the openings of the mask and, on the other hand, completely cover the non-hydrogenated rear face with a layer of aluminum (Al) 0.1-µm thick. At the end of this process, Schottky diodes of Au/P-Si structures were developed with a back contact of Al. The donor profile (electrically active) was obtained through *C–V* measurements at the frequency close to 1 MHz at room temperature by using a computer-assisted LCR meter, as shown in Fig. 2.

5. Results and discussions

5.1. Phosphorus deactivation and reactivation dependent on hydrogenation temperature and duration of the process

The deactivation and reactivation of phosphorus depend on duration of MW-ECR plasma hydrogenation. The influence of duration of MW-ECR plasma hydrogenation, varying from one to two hours, on the profiles of phosphorus in monocrystalline silicon ⟨100⟩ and of concentration $2\cdot10^{15}$ cm^{-3} was analyzed, at the process temperatures 50 to 500 °C, as shown in Figs 3a to 3e.

It is clear that the duration of hydrogenation used in this study has little influence on the depth of phosphorus deactivation, while the rate of neutralization is distinguished by the hydrogenation temperature. At $T = 50$ °C (Fig. 3a), formation of phosphorus-hydrogen complexes becomes saturated at the depth close to $X_e = 1.1$ µm after the treatment period of one hour. However, near the surface ($x \leq 1.1$ µm) there is a decrease in the doping profile depicting a reduced active phosphorus concentration, probably due to formation of phosphorus-hydrogen complexes during the hydrogenation of the films of monosilicon for two hours. We observe an increase in this profile over the depths $x \geq 1.1$ µm, giving rise to a flat distribution of phosphorus. Formation of PH complexes at 100 and 250 °C (Figs 3b to 3c) becomes saturated after a treatment period of one hour. At 400 °C (Fig. 3d), formation of PH increases, but it is slightly elevated for a hydrogenation period of two hours as compared to that of one hour. However, at 500 °C (Fig. 3e), the rate of phosphorus neutralization decreases, but it is even lower in hydrogenated films for one hour as compared to that of two hours. This observation can be explained by the reactivation of neutralized phosphorus atoms followed by PH bonds dissociation for one hour of hydrogenation treatment. In this process, the released hydrogen diffused out from silicon to the gas environment as reported earlier [26]. The depth to which the dopants are neutralized depends on the density of locations to which the hydrogen can bind the temperature and the duration of the treatment. For this, we have plotted variation of the inactive concentration of phosphorus [PH] measured at different depths of silicon as a function of the hydrogenation temperatures to examine the reactivation of phosphorus and the difficulty of diffusion of hydrogen into the bulk of silicon with the temperature increase. The results are shown in Fig. 4.

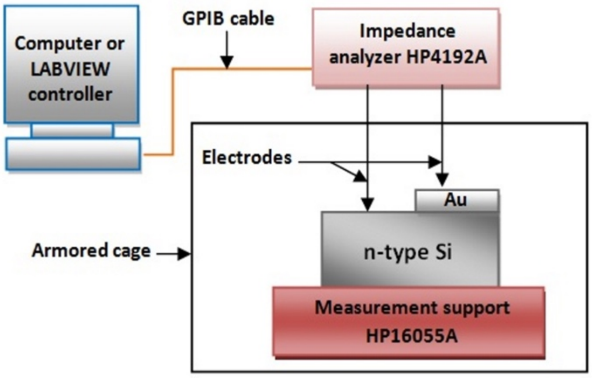

Fig. 2. Schematic of essential equipment used in *C–V* measurements of a Schottky diode.

Phosphorus deactivation rate at three different temperatures 50, 400 and 500 °C is observed to be high for hydrogenation treatment for one hour as compared to that for two hours, as shown in Figs 4a, 4b. At the temperatures of 100 and 250 °C, the rate of phosphorus deactivation decreases relatively. At the interface of Si Figs 4c–4e for $T < 400$ °C, a slightly reduced neutralization rate is observed for a hydrogenation period of two hours as compared to that of one hour. On the other hand, at $T = 400$ °C, the neutralization rate for the hydrogenation time of two hours is much higher as compared to that for one hour probably due to the high concentration of hydrogen atoms diffused into the bulk of silicon, since platelets do not form at this temperature. Finally, at $T = 500$ °C, the instability of PH complexes and subsequently their out-diffusion towards gaseous environment outweighs the mechanism of bulk diffusion to the detriment of a low rate of neutralization phosphorus.

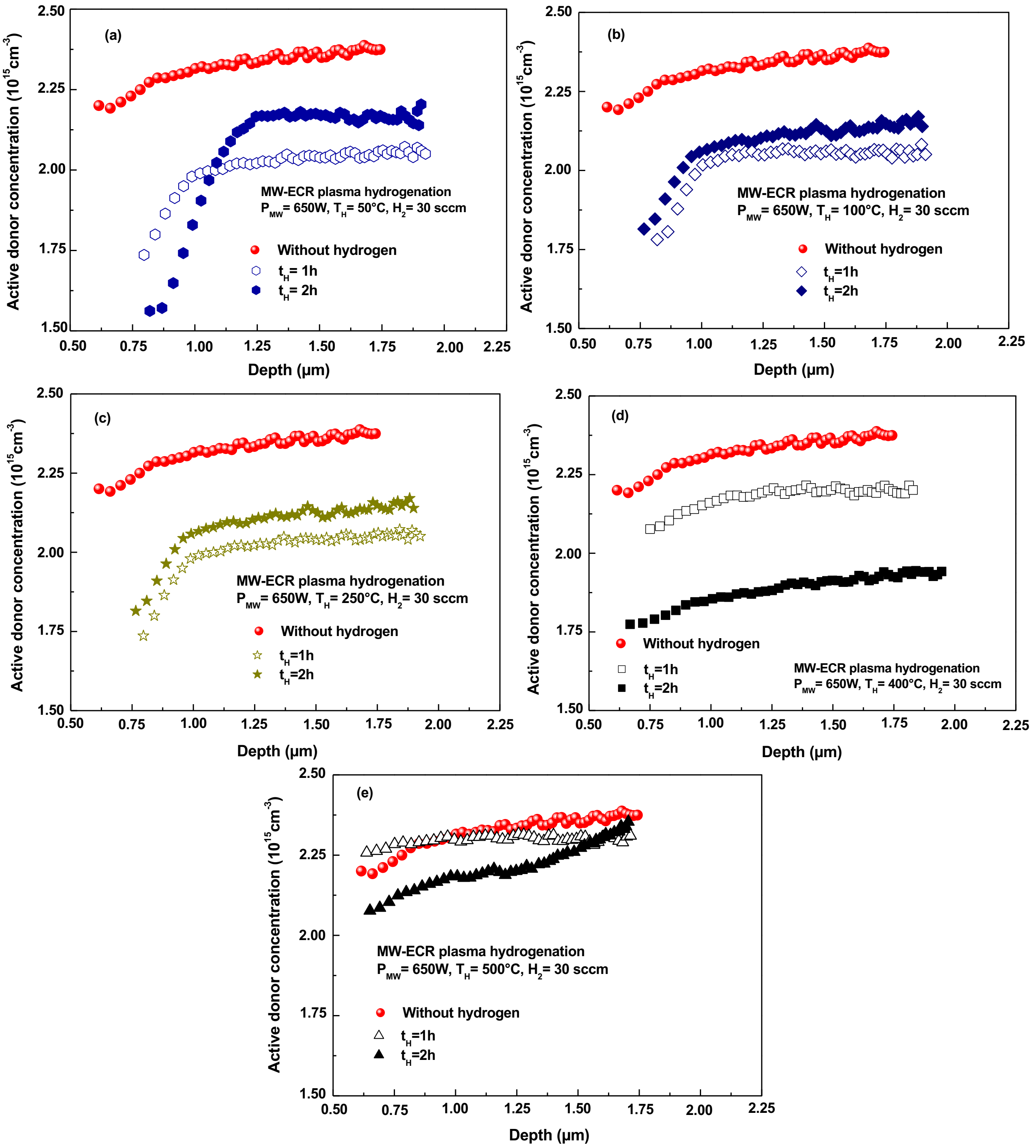

Fig. 3. Profile of active phosphorus concentration in hydrogenated Schottky diodes on FZ-Si doped at 10^{15} cm^{-3} for different temperatures.

Although the plasma composition of the MW-ECR system was not examined, it has been already reported that H^+ is the predominant type in hydrogen plasma [27]. The differences in the velocities of ions and electrons give rise to the electrostatic sheath, with the contrasting magnetic field, induce the movement of H^+ ions towards the surface of the sample, in contact with the plasma [28]. Numerous studies [29, 30] have shown that hydrogen really exists in three associated states of charge, (H^+, H^0 and H^-), and it is in its atomic form mobile in silicon at room temperature and highly reactive. Formation energies of these three states of charge depend on the position of Fermi level within the forbidden band [31]. In *n*-type silicon, the H^- charge state is favored and acts as an electron acceptor [32]. The work of Reizk *et al.* [33] has shown that the confinement of atomic hydrogen defaults in particular by phosphorus atoms and the disappearance of atomic hydrogen due to formation of hydrogen molecules. Likewise, the neutral hydrogen H^0 configuration does not appear to be energy stable, whatever the position of the Fermi level. Neutralization of phosphorus in crystalline silicon occurs preferentially

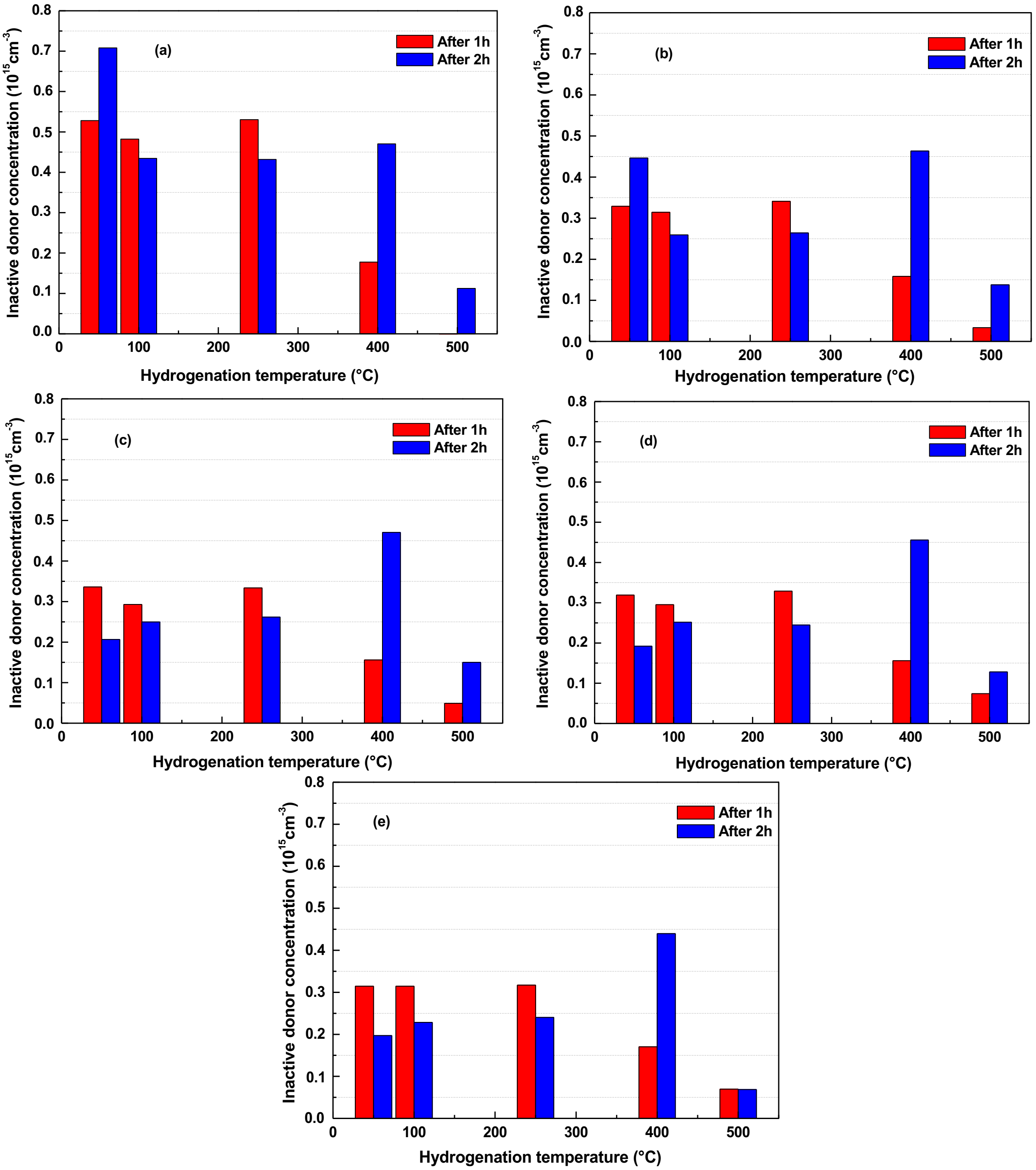

Fig. 4. Inactive phosphorus concentration *vs* hydrogenation temperature at the depths d (μm): 0.8 (a), 1.0 (b), 1.2 (c), 1.4 (d), 1.6 (e).

via H^- ions. For this reason, a large part of hydrogen H^+ from the plasma is converted first into H^0 by gaining one electron ($H^+ + e^- \rightarrow H^0$) and then into H^- after gaining another electron ($H^0 + e^- \rightarrow H^-$), moreover, due to Colombian attraction forces, H^- ions are attracted to ionized donor P^+ atoms to give rise to neutral complexes ($H^- + P^+ \rightarrow PH$), therefore, this causes a decrease in the electrical activity of dopants [34]. Molecular hydrogen H_2 has been proposed by some experimental studies [35, 36] to play an important role in the diffusion of hydrogen in Si and the complex reactions of hydrogen with dopants. During the process of hydrogen H^0 formation, the latter can diffuse into silicon bulk or can interact with another H^0 to create the hydrogen molecule ($H^0 + H^0 \rightarrow H_2$) [37]. This latter possibility is widely favored following the very weak diffusion of H^0 in silicon as compared to those of H^+ and H^- ions [38]. Other studies [39, 40] have shown that the molecular hydrogen H_2 appears in platelets located in the lower layer near the silicon surface. Similar results were obtained by Huang *et al.* [41]. The observations revealed that the size of these platelets depends on hydrogen diffusivity in silicon, although the platelet formation reduces the hydrogen diffusivity.

Table 1. Hydrogen diffusion coefficients at different hydrogenation temperature and duration of the process.

	$t_H = 1$ h		$t_H = 2$ h	
T_H-, °C	X_e, µm	D_{H^-}, cm²/s	X_e, µm	D_{H^-}, cm²/s
50	0.7835	$1.7052 \cdot 10^{-12}$	0.8020	$8.933 \cdot 10^{-12}$
100	0.7960	$1.7600 \cdot 10^{-12}$	0.7433	$1.5347 \cdot 10^{-12}$
250	0.7804	$1.6917 \cdot 10^{-12}$	0.7558	$7.933 \cdot 10^{-12}$
400	0.7342	$1.4973 \cdot 10^{-12}$	0.6538	$5.936 \cdot 10^{-12}$
500	0.6137	$1.0461 \cdot 10^{-12}$	0.6173	$5.294 \cdot 10^{-12}$

This phosphorus passivation by hydrogen is governed by not only the chemical reactions between two species but also by different phenomena like hydrogen diffusivity in the bulk as H^- and favors the chemical reactions to obtain the PH complexes. The diffusion coefficients corresponding to the depth X_e have been calculated by relation (7) to prove these arguments. The results are listed in Table 1.

It has been observed that for a hydrogenation period of one hour, a relatively higher coefficient of hydrogen diffusion is obtained as compared to that for two hours, which resulted in deep hydrogen penetration into silicon films as it is confirmed by *C–V* measurements. These results are strongly correlated with those reported earlier [30, 42].

5.2. Effect of thermal annealing under forming gas

Thermal annealing in the FG environment and presence of ambient molecular H_2 provide deep diffusion of hydrogen, since the diffusivity of molecular hydrogen is known to be extremely low, so it is nevertheless essential for diffusion of hydrogen inside the bulk of Si and subsequent passivation there. In this section, the influence of thermal annealing under the forming gas, which annealing temperature was varied from 100 to 700 °C for 1 hour, on active phosphorous in hydrogenated samples at 400 °C for one hour. Figs 5a, 5b show the depth profiles for the active donor concentration in the FZ-Si Schottky diodes at different annealing temperatures.

It is clear from Fig. 5a that reduction in active phosphorus concentration at all depths takes place with the increase in the annealing temperature up to 400 °C, which means that for the same quantity of hydrogen diffused in monosilicon, the concentration of deactivated phosphorus is pronounced for higher annealing temperatures. However, Fig. 5b shows that after annealing at 500 °C, the increase in the profile for the depths < 1 µm indicated that annealing accelerated dissociation of PH complexes in the region close to the surface with a slight increase in the bulk activated donor concentration. Whereas higher annealing temperatures again result in deactivation rate values close to the non-hydrogenated test profile. This can be attributed to the desorption of hydrogen at temperatures above 600 °C, indicating the breaking of a large part of the PH bonds present at the interface or on the surface of the samples.

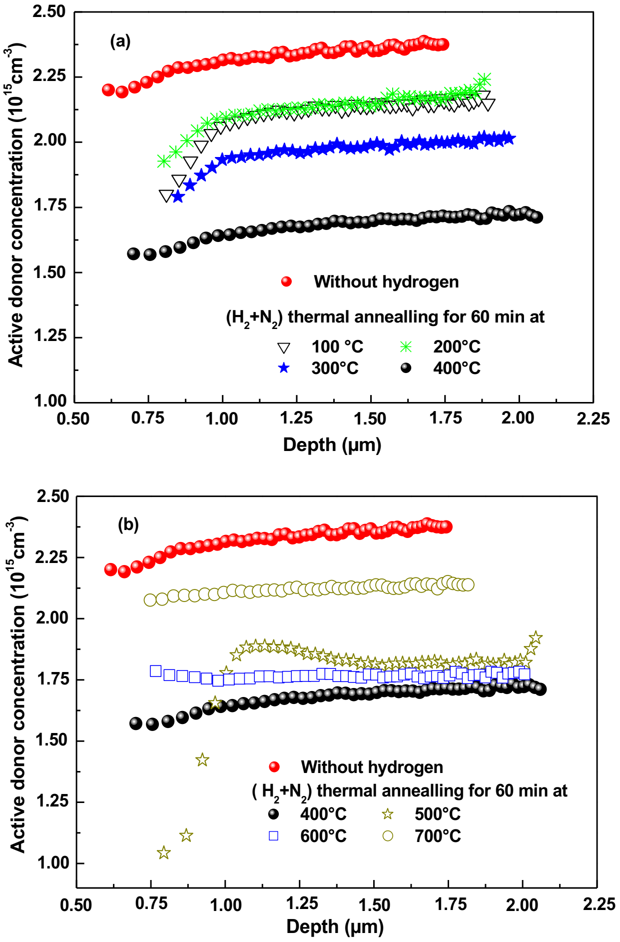

Fig. 5. Active donor concentration profiles as a function of depletion depth at various annealing temperatures.

The obtained results show that the thermal dissociation of PH complexes is strongly described by the $PH = P^+ + H^-$ reaction and therefore the unambiguous existence of H^- species in *n*-type silicon. Moreover, the effect of high annealing temperature is probably remarkable on the dissociation rate of PH complexes observed in Schottky diodes.

Fig. 6 validates the arguments made in the previous paragraphs. Indeed, the low deactivation rates obtained between 100 and 300 °C results from hydrogen diffusion in the silicon bulk. This hydrogen is trapped in platelets close to the surface of silicon. At the annealing temperature 400 °C, the absence of platelets close to the surface resulted in high deactivation rates and consequently, diffusion of maximum hydrogen atoms in the bulk gives rise to the saturation of PH complexes. However, for the annealing temperatures 500 and 600 °C, instability of PH complexes observed due to out-diffusion of hydrogen in the gaseous environment leads to the detriment of a slight decrease in the rate of phosphorus neutralization. Finally, the low rate of phosphorus neutralization was obtained at the temperature 700 °C mainly due to the out-diffusion of hydrogen and dissociation of PH complexes. This result is similar with the results reported in [42, 43].

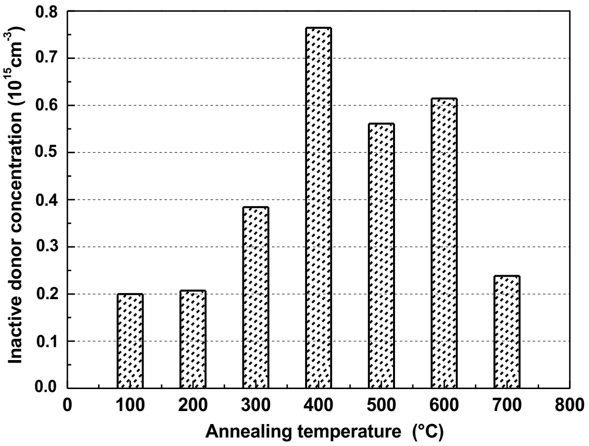

Fig. 6. Inactive donor concentration at the depth close to 1.6 μm as a function of annealing temperature.

Indeed, it is accepted that annealing under gas flow can cause the adsorption of gas molecules. The probability for this adsorption to occur on the surface of a single crystal at room temperature is low, the hydrogen molecules must be first dissociated for adsorption to occur by working at the temperatures > 200 °C. This absorption phenomenon is all the more marked in doped silicon, given the emergence of dopants on the surface, which accentuates the absorption surface and accelerates penetration of hydrogen [44]. After implantation and diffusion into silicon, hydrogen is present in its atomic form and can bind to a dopant or segregate on interstitials. Citing Ben Amor *et al.* [45], diffusion of hydrogen, passivation by hydrogen could result in formation of Si–H or Si–H_2 complexes. This behavior indicates that the treatment of sample in substrate temperature of 350 °C reduces hydrogenation of the deposited films, which suggests that at high temperatures the energy at the surface of substrate reduces the stability of Si–H bonds and Si–H_2. The saturation of pendant bonds with hydrogen has of course been proposed, but it is not compatible with the instability of the bonds observed during annealing at temperatures above 400 °C. The analyzed profiles of hydrogen in silicon validate the argument that at a higher annealing temperature, higher quantity of hydrogen atoms diffuses into the silicon lattice, and silicon exposure to the hydrogen plasma within the temperature range 100 to 250 °C results in formation of platelets. Formation of these defects also manages to make effective barriers to prevent diffusion of hydrogen into the silicon bulk during thermal annealing. Literature suggests that, for the annealing temperature close to 250 °C, the low density of platelets is achieved and, for temperatures around 450 °C, the low efficiency of the phosphorous neutralization is reached [46, 47]. N.M. Johnson *et al.* explained the instability of PH complexes and out-diffusion of hydrogen atoms although linked to the dopant by Coulomb attraction [48]. The obvious interpretation of the profiles observed at very high temperatures ($T \geq 500$ °C) is the release of monoatomic hydrogen during thermal dissociation of PH complexes, which undergoes a weak drift force compared to a clearly significant drift from the surface. Migration of H^0 species may not contribute towards evolution of the profiles, however, migration of dissociated hydrogen as H^- simply explains the behavior of PH complex recombination observed in Si bulk [49, 50].

5.3. Diffusion of hydrogen under annealing with the forming gas

Considered in this section is a view of the hydrogen diffusion coefficient (D_{H^-}) under a FG atmosphere and its dependence on the annealing temperature. Table 2 shows the calculated diffusion coefficient values of our samples corresponding to the depth (X_e) by using the relation (7).

It is observed that a high hydrogen diffusion coefficient is obtained for samples at the annealing temperature $T = 300$ °C, which confirms deep penetration of hydrogen H into the bulk of our silicon films registered in our *C–V* measurements. A low hydrogen diffusion coefficient was obtained for the samples at 400 °C. This phenomenon is mainly caused by the rate of combination between hydrogen and phosphorus, to form electrically inactive complexes (PH), which attains its maximum at this temperature, as already mentioned above (Fig. 6). Through these observations on the values of the diffusion coefficients, we can clearly explain the mechanism of hydrogen diffusion under FG environment, which can take the following three phases: dissociation of the gas molecules at the surface temperatures above 200 °C, adsorption of the hydrogen atoms thus released by the surface of the crystal and diffusion in the bulk, and hydrogen can also combine with phosphorus to form electrically inactive (PH) complexes that are unstable at the annealing temperatures above 500 °C, and subsequently their out-diffusion to the gaseous atmosphere prevails over the mechanism of bulk diffusion, and consequently weak formation of the PH complexes takes place. In this stage, our results greatly contribute to answer the question raised in Ref. [51] regarding the annealing in FG which is: how the annealing in FG, the molecular perimeter of H, led it to a deep diffusion of H given the fact that the diffusion of molecular hydrogen is known to be very low?

Finally, the values of the obtained diffusion coefficients are of the same order of magnitude as those cited in Refs. [30, 42].

Table 2. Hydrogen diffusion coefficients at different annealing temperatures (T_a).

T_{H^-}, °C	X_e, μm	D_{H^-}, cm^2/s
100	0.7957	$1.7587 \cdot 10^{-12}$
200	0.7928	$1.7459 \cdot 10^{-12}$
300	0.8561	$2.0358 \cdot 10^{-12}$
400	0.6839	$1.2992 \cdot 10^{-12}$
500	0.7777	$1.6800 \cdot 10^{-12}$
600	0.7656	$1.6281 \cdot 10^{-12}$
700	0.7052	$1.4766 \cdot 10^{-12}$

6. Conclusion

Revealed in this work is the effect of thermal annealing ambiance on phosphorus passivation and reactivation in the silicon-based Schottky diodes, and it shows that hydrogen deactivates phosphorus at a particular annealing temperature. After saturation, a further increase in annealing temperature reactivates phosphorus in the starting material. The analysis reveals that hydrogen diffusion in silicon causes the neutralization of phosphorus and can even produce hydrogen molecules forming platelets close to the silicon surface at hydrogenation temperatures between 50 and 100 °C, and subsequent diffusion of hydrogen in the bulk weakens. Moreover, it has been observed that the phosphorus passivation rate remains homogeneous over all the depths measured at T = 400 °C. The thermal annealing in forming gas indicates that the phosphorus passivation rate increases with the annealing temperature up to saturation at 400 °C. At high temperatures, a decrease in the concentration of PH complexes due to their dissociation leads to reactivation of phosphorus under thermal treatment. Consequently, at this stage, the mechanisms of passivation and reactivation of phosphorus in silicon have been ascertained.

Acknowledgment

The authors would like to acknowledge the personnel at ICUBE (Formerly InESS) Laboratory for their support and cooperation.

References

1. Johnson N.M., Moyer M.D. Absence of oxygen diffusion during hydrogen passivation of shallow acceptor impurities in single crystal silicon. *Appl. Phys. Lett.* 1985. **46**. P. 789–787. http://dx.doi.org/10.1063/1.95883.
2. Kitajima M., Ishioka K., Nakanoya K. *et al.* Three different forms of hydrogen molecules in silicon. *Jpn. J. Appl. Phys.* 1999. **38**. P. L691–L693. http://iopscience.iop.org/1347-4065/38/7A/L691.
3. Jadhavar A., Pawbake A., Waykar R. *et al.* Influence of RF power on structural optical and electrical properties of hydrogenated nano-crystalline silicon (nc-Si:H) thin films deposited by PE-CVD. *J. Mater. Sci.: Mater. Electron.* 2016. **27**. P. 12365–12373. https://doi.org/10.1007/s10854-016-5024-1.
4. Dail X., Cai H., Zhang D. *et al.* Annealing induced amorphous/crystalline silicon interface passivation by hydrogen atom diffusion. *J. Mater. Sci.: Mater. Electron.* 2016. **27**. P. 705–710. https://doi.org/10.1007/s10854-015-3806-5.
5. Gotoha K., Wilde M., Ogura S. *et al.* Impact of chemically grown silicon oxide interlayers on the hydrogen distribution at hydrogenated amorphous silicon/crystalline silicon heterointerfaces. *Appl. Surf. Sci.* 2021. **567**. P. 150799. https://doi.org/10.1016/j.apsusc.2021.150799.
6. Chena T.C., Yub I.S., Yang Z.P. Hydrogenation behaviors in passivated emitter and rear silicon solar cells with variously hydrogenated SiN_x films. *Appl. Surf. Sci.* 2020. **521**. P. 146386. https://doi.org/10.1016/j.apsusc.2020.146386.
7. Hallam B.J., Hamer P.G., Ciesla A.M. *et al.* Development of advanced hydrogenation processes for silicon solar cells *via* an improved understanding of the behaviour of hydrogen in silicon. *Prog. Photovolt. Res. Appl.* 2020. **28**, No 1. P. 3240. https://doi.org/10.1002/pip.3240.
8. Abdurrazaq A., Raji A.T., Meyer W.E. *Ab initio* study of the effect of hydrogen passivation on boron-oxygen-carbon related defect complexes in silicon. *Mater. Sci. Semicond. Process.* 2020. **110**. P. 104967. https://doi.org/10.1016/j.mssp.2020.104967.
9. Vidhya Y.E.B., Vasa N.J. Enhanced electrical characteristics of a-Si thin films by hydrogen passivetion with Nd^{3+}:YAG laser treatment in under water for photovoltaic applications. *Appl. Phys. A.* 2017. **123**. P. 528. https://doi 10.1007/s00339-017-1130-z.
10. Pal S., Barrirero J., Lehmann M. *et al.* Quantification of hydrogen in nanostructured hydrogenated passivating contacts for silicon photovoltaics combining SIMS-APT-TEM: A multiscale correlative approach. *Appl. Surf. Sci.* 2021. **555**. P. 149650. https://doi.org/10.1016/j.apsusc.2021.149650.
11. Sharma R., Chong A.P., Lib J.B. *et al.* Role of post-metallization anneal sequence and forming gas anneal to mitigate light and elevated temperature induced degradation of multicrystalline silicon solar cells. *Solar Energy Materials and Solar Cells*. 2019. **195**. P. 160–167. https://doi.org/10.1016/j.solmat.2019.02.036.
12. Reynolds N.D., Panda C.D., Essick J.M. Capacitance-voltage profiling: Research-grade approach versus low-cost alternatives. *Am. J. Phys.* 2014. **82**, No 3. P. 196–205. http://dx.doi.org/10.1119/1.4864162.
13. Rahman Md.M., Udoy A.B. Investigation of surface passivation schemes for *p*-type monocrystalline silicon solar cell. *Appl. Phys. A.* 2016. **122**. P. 926. https://doi 10.1007/s00339-016-0434-8.
14. Chena D., Hamer P.G., Kima M. *et al.* Hydrogen induced degradation: A possible mechanism for light- and elevated temperature-induced degradation in *n*-type silicon. *Solar Energy Materials and Solar Cells*. 2018. **185**. P. 174–182. https://doi.org/10.1016/j.solmat.2018.05.034.
15. Wu Z., Zhang L., Liu W. *et al.* Role of hydrogen in modifying a-Si:H/c-Si interface passivation and band alignment for rear-emitter silicon heterojunction solar cells. *J. Mater. Sci.: Mater. Electron.* 2020. **31**. P. 9468–9474. https://doi.org/10.1007/s10854-020-03486-5.
16. You J., Liu H., Qu M. *et al.* Hydrogen-rich c-Si interfacial modification to obtain efficient passivation for silicon heterojunction solar cell. *J. Mater. Sci.: Mater. Electron.* 2020. **31**. P. 14608–14613. https://doi.org/10.1007/s10854-020-04023-0.

17. Bao S., L.Yang L., J. Huang J. *et al.* The rapidly reversible processes of activation and deactivation in amorphous silicon heterojunction solar cell under extensive light soaking. *J. Mater. Sci.: Mater. Electron.* 2021. **32**. P. 4045–4052. https://doi.org/10.1007/s10854-020-05146-0.
18. Yang P., Zeng X. Effect of hydrogenated silicon film microstructure on the surface states of *n*-type silicon nanowires and solar cells. *J. Mater. Sci.: Mater. Electron.* 2021. **32**. P. 3066–3071. https://doi.org/10.1007/s10854-020-05056-1.
19. Lee S.H., Bhopal M.F., Lee D.W. *et al.* Review of advanced hydrogen passivation for high efficient crystalline silicon solar cells. *Mater. Sci. Semicond. Process.* 2018. **79**. P. 66–73. https://doi.org/10.1016/j.mssp.2018.01.019.
20. Sharma R., Chong A.P., Li J. B. *et al.* Role of post-metallization anneal sequence and forming gas anneal to mitigate light and elevated temperature induced degradation of multicrystalline silicon solar cells. *Solar Energy Materials and Solar Cells*. 2019. **195**. P. 160–167. https://doi.org/10.1016/j.solmat.2019.02.036.
21. Yadav T.S., Sharma A.K., Kottantharayil A. *et al.* Comparative study of different silicon oxides used as interfacial passivation layer (SiN_y:H/SiO_x/n^+-Si) in industrial monocrystalline silicon solar cells. *Solar Energy Materials and Solar Cells*. 2019. **201**. P. 110077. https://doi.org/10.1016/j.solmat.2019.110077.
22. Belfennache D., Madi D., N. Brihi N. *et al.* Mechanism for phosphorus deactivation in silicon-based Schottky diodes submitted to MW-ECR hydrogen plasma. *Appl. Phys. A*. 2018. **124**. P. 697. https://doi.org/10.1007/s00339-018-2118-z.
23. Letty E., Veirman J., Favre W. *et al.* Bulk defect formation under light soaking in seed-end *n*-type Czochralski silicon wafers – Effect on silicon heterojunction solar cells. *Solar Energy Materials and Solar Cells*. 2017. **166**. P. 147–156. https://doi.org/10.1016/j.solmat.2017.03.019.
24. Chatbouri S., Troudi M., Kalboussi A. *et al.* Interface traps contribution on transport mechanisms under illumination in metal–oxide–semiconductor structures based on silicon nanocrystals. *Appl. Phys. A*. 2018. **124**. P. 114. https://doi.org/10.1007/s00339-017-1533-x.
25. Vinod P.N. The capacitance–voltage measurement of the screen-printed silicon solar cells with electrochemically etched nanostructured porous silicon antireflection coating. *J. Mater. Sci.: Mater. Electron.* 2013. **24**. P. 1395–1404. https://doi.org/10.1007/s10854-013-1145-y.
26. Barakel D., Ulyashin A., Périchaud I. *et al.* *n–p* Junction formation in *p*-type silicon by hydrogen ion implantation. *Solar Energy Materials and Solar Cells*. 2002. **72**. P. 285–290. https://doi.org/10.1016/S0927-0248(01)00176-3.
27. Somana A., Antony A. A critical study on different hydrogen plasma treatment methods of a-Si:H/c-Si interface for enhanced defect passivation. *Appl. Surf. Sci.* 2021. **553**. P. 149551. https://doi.org/10.1016/j.apsusc.2021.149551.
28. Yoon S.F., Tan K.H., Zhang Q. *et al.* Effect of microwave power on the electron energy in electron cyclotron resonance plasma. *Vacuum.* 2001. **61**. P. 29–35. https://doi:10.1016/s0042-207x(00)00429-2.
29. Velichko O.I., Shaman Y.P., Kovaliova A.P. Simulation of hydrogen diffusion and boron passivation in crystalline silicon. *Modelling Simul. Mater. Sci. Eng*. 2014. **22**. P. 035003. https://doi:10.1088/0965-0393/22/3/035003.
30. Chen D., Hamer P., Kim M. *et al.* Hydrogen-induced degradation: Explaining the mechanism behind light- and elevated temperature-induced degradation in *n*- and *p*-type silicon. *Solar Energy Materials and Solar Cells*. 2020. **207**. P. 110353. https://doi.org/10.1016/j.solmat.2019.110353.
31. Nickel N.H. Hydrogen transport in doped and undoped polycrystalline silicon. *Microelectronics Reliability*. 2007. **47**. P.899–902. https://doi.org/10.1016/j.microrel.2006.10.014.
32. Song L., Wenham A., Wang S. *et al.* Laser enhanced hydrogen passivation of silicon wafers. *Int. J. Photoenergy*. 2015. **122**. ID 193892. https://doi.org/10.1155/2015/193892.
33. Rizk R., de Mierry P., Ballutaud D. *et al.* Hydrogen diffusion and passivation processes in *p*- and *n*-type crystalline silicon. *Phys. Rev. B.* 1991. **44**. P. 6141–6151. http://doi:10.1103/physrevb.44.6141.
34. Herring C., Johnson N.M., Chiris G. *et al.* Energy levels of isolated interstitial hydrogen in silicon. *Phys. Rev. B.* 2001. **12**. P. 125209. https://doi:10.1103/physrevb.64.125209.
35. Choi S.J., Yu G.J., Kang G.H. *et al.*The electrical properties and hydrogen passivation effect in mono crystalline silicon solar cell with various pre-deposition times in doping process. *Renewable Energy*. 2013. **54**. P. 96–100. https://doi.org/10.1016/j.renene.2012.08.052.
36. Stavola M., Kleekajai S., Wen L. *et al.* IR characterization of hydrogen in crystalline silicon solar cells. *Phys. B: Condens. Matter*. 2009. **404**. P. 5066–5070. https://doi.org/10.1016/j.physb.2009.08.226.
37. Lavrov E.V., Hiller M., Weber J., Raman scattering on H_2 in platelets in silicon. *Phys. B: Condens. Matter*. 2009. **404**. P. 5085–5088. https://doi.org/10.1016/j.physb.2009.08.249.
38. Ohmi H., Kimoto K., Nomura T. *et al.* Study on silicon removal property and surface smoothing phenomenon by moderate-pressure microwave hydrogen plasma. *Mater. Sci. Semicond. Process*. 2021. **129**. P. 105780. https://doi.org/10.1016/j.mssp.2021.105780.

39. Dürr M., Höfer U. Hydrogen diffusion on silicon surfaces. *Prog. Surf. Sci.* 2013. **88**. P. 61–101. https://doi.org/10.1016/j.progsurf.2013.01.001.
40. Chaoa D.S., Hsiaob Y.C., Liang J.H. *et al.* Effects of crystal plane orientation on blistering kinetics and defect evolution in silicon implanted by hydrogen molecular ions. *Surface and Coatings Technology*. 2020. **394**. P. 125872. https://doi.org/10.1016/j.surfcoat.2020.125872.
41. Huang Y.L., Ma Y., Job R. *et al.* Suppression of hydrogen diffusion at the hydrogen-induced platelets in *p*-type Czochralski silicon. *Appl. Phys. Lett.* 2005. **86**. P 131911. https://doi.org/10.1063/1.1896443.
42. Belfennache D., Brihi N., Madi D. Effective phosphorus deactivation in Schottky diodes hydrogenated in MW-ECR plasma reactor. *2016 8th International Conference on Modelling, Identification and Control (ICMIC)*, 2016. P. 497–502. https://doi:10.1109/icmic.2016.7804164.
43. Schutz-Kuchly T., Slaoui A. Double layer a-Si:H/ SiN:H deposited at low temperature for the passive-tion of *n*-type silicon. *Appl. Phys. A*. 2013. **112**. P. 863–867. https://doi.org/10.1007/s00339-013-7802-4.
44. Weber J., Knack S., Feklisova O.V. *et al.* Hydrogen penetration into silicon during wet-chemical etching. *Microelectron. Eng.* 2003. **66**. P. 320–326. https://doi.org/10.1016/S0167-9317(02)00926-7.
45. Amor S.B., Atyaoui M., Bousbih R. *et al.* Effect of substrate temperature on microstructure and optical properties of hydrogenated nanocrystalline Si thin films grown by plasma enhanced chemical vapor deposition. *Solar Energy*. 2014. **108**. P. 126–134. https://doi.org/10.1016/j.solener.2014.06.024.
46. Fukata N., Sato S., Fukuda S. *et al.* Passivation and reactivation of carriers in B- and P-doped Si treated with atomic hydrogen. *Phys. B: Condens. Matter.* 2007. **401-402**. P. 175–178. https://doi.org/10.1016/j.physb.2007.08.140.
47. Fukata N., Sato S., Morihiro H. *et al.* Dopant dependence on passivation and reactivation of carrier after hydrogenation. *J. Appl. Phys.* 2007. **101**. P. 46107. https://doi.org/10.1063/1.2654831.
48. Meddeb H., Bearda T., Abdelwahab I. *et al.* Thermal, structural and electrical study of the effect of annealing on the passivation by amorphous silicon of *n*-type crystalline (100) silicon surfaces. *Energy Procedia.* 2014. **55**. P. 818–826. https://doi.org/10.1016/j.egypro.2014.08.065.
49. Johnson N.M., Herring C., Van de Walle C.G. Inverted order of acceptor and donor levels of monatomic hydrogen in silicon. *Phys. Rev. Lett.* 1994. **73**. P. 130. https://doi:10.1103/physrevlett.74.1889.
50. Johnson N.M., Herring C. Diffusion of negatively charged hydrogen in silicon. *Phys. Rev. B.* 1992. **46**, Issue 23. P. 15554–15557. https://doi.org/10.1103/ physrevb.46.15554.
51. Madi D., Focsa A., Roquesa S. *et al.* Effect of MW-ECR plasma hydrogenation on polysilicon films based solar cells. *Energy Procedia*. 2010. **2**. P. 151–157. https://doi.org/10.1016/j.egypro.2010.07.021.

Authors and CV

Djamel Eddine Belfennache, born in 1987, defended his PhD Thesis in physics (semiconductor physics) in 2019 at the Faculty of Exact Sciences and Technology of the University of Mohamed Seddik Ben Yahia Jijel in Algeria. He is a senior researcher in the Department of Materials and Surface Structure at the Research Center for Industrial Technologies in Algeria. He authored 4 articles and participated in several international conferences in Turkey, Spain and France. His field of scientific interests include physics and technology of semiconductor materials, solar cells, as well as nanostructures and ferromagnetic materials.
E-mail: d.belfenache@crti.dz;
belfennachedjamel@gmail.com

Djamal Madi, born in 1973, he defended his PhD Thesis in electronics for the year 2012 at the Faculty of Exact Sciences and Technology at the University of Mohamed Seddik Ben Yahia Jijel in Algeria. Professor at the Faculty of Science and Technology at the University of Bouira in Algeria. He held several positions in the field of higher education and scientific researches. He supervised several research projects and supervised PhD students. He authored 10 articles and participated in many international conferences in Turkey, Belgium and France. His scientific interests include semiconductor materials technology, solar cells, as well as renewable energies.
E-mail: madidjamel@yahoo.com

Radhia Yakhlef, born in 1979, PhD student. She works at the Faculty of Exact Sciences and Technology at the University of Farhat Abbas Setif in Algeria. She acts as a research attaché in the Department of Materials and Surface Structure at the Scientific Research Center for Industrial Technologies in Algeria. Radhia Yakhlef has participated in many research projects, as well as in many international conferences in Turkey. Her scientific interests include electrochemistry, corrosion, modified electrodes, and renewable energies.
E-mail: r.yekhlef@crti.dz; ryekhlef@yahoo.fr

Linda Toukal, born in 1975, defended PhD Thesis in electrochemistry in 2018 at the Faculty of Exact Sciences and Technology, University of Farhat Abbas Setif, Algeria. She is a Professor at the Faculty of Science and Technology at the University of Setif in Algeria. She has participated in many research projects, established several partnerships with Moroccan universities, written 3 articles, and participated in many international conferences in Turkey and Morocco. Her scientific interests include electrochemistry, corrosion, modified electrodes, and renewable energies. E-mail: ltoukal@yahoo.fr

Naima Maouche, born in 1973, defended her PhD Thesis in electrochemistry in 2009 at the Faculty of Technology at Farhat Abbas Setif University in Algeria. Professor at the Department of Processes Engineering, Faculty of Technology at the University of Setif-1 in Algeria. She held several positions in the field of higher education and scientific researches. N. Maouche supervised several research projects and supervised PhD students. She held several partnerships with French universities, authored 24 articles, and participated in many international conferences in Tunisia, Turkey and France. Her scientific interests include electrochemistry, conductive polymers, modified electrodes, nanocomposites and renewable energies. E-mail: m_naima2001@yahoo.fr; nmaouche@univ-setif.dz

M. Saeed Akhtar, born in 1981, defended his PhD thesis in Microelectronics/Nanotechnology in 2015 at the Centre of Excellence in Solid State Physics, University of the Punjab, Lahore, Pakistan. He is working as Assistant Professor (TTS) at the Department of Physics, Division of Science and Technology, University of Education, Lahore, Pakistan. He has authored more than fifteen research papers in impact factor journals for the recent five years. He has also supervised 15 MS and 12 MSc/BS students by 2021. The area of his scientific interests includes materials science and specifically nano-structures/thin films.
E-mail: saeed.akhtar@ue.edu.pk;
https://orcid.org/0000-0003-2431-9932.

Swat Zahra, born in 1976, defended her PhD Thesis in physics (high energy physics) in 2012 at the High Energy Physics Center of Punjab University, Lahore. She held several positions in the field of higher education and scientific research and supervised several theses for High Energy Physics University of the Punjab, Lahore. She has authored 12 articles and participated in several international forums. Her field of scientific interests include particle physics, mathematical methods of physics, quantum mechanics relativity and cosmology, modern physics. E-mail: sarwat.zahra@ue.edu.pk; https://orcid.org/0000-0001-8901-6639.

Вплив атмосфери при термічному відпалі на механізми пасивації та реактивації фосфору в діодах Шотткі на основі кремнію, гідрогенізованих плазмою мікрохвильового циклотронного електронного резонансу

D. Belfennache, D. Madi, R. Yekhlef, L. Toukal, N. Maouche, M.S. Akhtar, S. Zahra

Анотація. Основною метою даної роботи є дослідження впливу термічного відпалу при утворенні газової атмосфери на механізми дезактивації та реактивації фосфору в діодах Шотткі на основі кремнію. По-перше, потужність мікрохвильової плазми, початкова концентрація фосфору у зразках та потік водню були зафіксовані відповідно 650 Вт, 10^{15} см$^{-3}$ та 30 куб. см для дослідження поведінки різних робочих параметрів діодів, зокрема тривалості та температури гідрогенізації. По-друге, декілька зразків, гідрогенізованих при 400 °C протягом 1 години, відпалювались в атмосфері формуючого газу (10% H_2 + 90% N_2) у діапазоні температур від 100 до 700 °C протягом 1 години. Профілі концентрації активного фосфору контролювали шляхом оцінки зміни концентрації фосфору після гідрогенізації або термічного відпалу в середовищі формуючого газу шляхом вольт-ємнісних вимірювань. У результаті отримано значення температури та тривалості гідрогенізації, що в кінцевому підсумку продемонструвало складну поведінку фосфору та водню в кремнії. Однак швидкість пасивації фосфору є однорідною на всіх глибинах, виміряних при 400 °C. Термічний відпал у формуючому газі свідчить про збільшення швидкості пасивації фосфору як функції температури відпалу, поки швидкість пасивування не досягне насичення у зразку, відпаленому при 400 °C. При більш високих температурах спостерігається зменшення концентрації фосфорно-водневих комплексів через дисоціацію цих комплексів та реактивацію фосфору під дією теплового впливу.

Ключові слова: пасивація фосфору, гідрогенізація плазмою, термічний відпал, формуючий газ.